Volume 8, Issue 4, 2019, 711 - 714 **ISSN 2284-6808**

Letters in Applied NanoBioScience

https://nanobioletters.com/

https://doi.org/10.33263/LIANBS84.711714

Original Research Article **Open Access Journal**

Received: 25.09.2019 / Revised: 22.10.2019 / Accepted: 25.10.2019 / Published on-line: 28.10.2019

Ultrasonic application and spray drying during amorphous calcium phosphate synthesis

Jorge E. Rodriguez Chanfrau [1,*], Yaymarilis Veranes Pantoja [2], Antonio Carlos Guastaldi [1]

[1]Institute of Chemistry, Paulista State University, Araraquara, Brazil

[2]Center of Biomaterials, University of Havana. Vedado, La Habana, Cuba

*corresponding author e-mail address: ***jerodriguez354@gmail.com*** | Scopus ID 7801488065

ABSTRACT

Hydroxyapatite, amorphous calcium phosphates, calcium triphosphate and calcium octaphosphate are the main components present in bones and teeth. Calcium phosphates are easily synthesized, playing an important role in regenerative medicine, being able to be used as bone implants. There are different ways of synthesizing phosphates, the most commonly used being wet chemical method. The objective of this work was to study the influence of the use of ultrasound and spray drying on the synthesis of amorphous calcium phosphate. Two synthetic variants were studied. One without ultrasound application and the other with ultrasound application. The samples obtained were characterized by X-ray diffraction, FTIR spectroscopy and scanning electron microscopy. The particle size by electron microscopy and the calcium content by atomic absorption was determined. The results showed that when spray drying is applied, particle sizes of less than 261 nm are obtained in the samples synthesized without ultrasound application, being less than 59 nm in the samples synthesized with ultrasound application. The statistical analysis by ANOVA showed significant differences between the particle sizes of the samples synthesized without ultrasound application and the samples synthesized by applying ultrasound. In both cases the particles were spherical. The results obtained show that the application of ultrasound during the synthesis process decreases the particle size, increasing the surface area, which favors the spray drying process.

Keywords: *Amorphous calcium phosphate; Spray drying; Biomaterials; Particle size.*

1. INTRODUCTION

Hydroxyapatite, amorphous calcium phosphates, calcium triphosphate and calcium octaphosphate are the main components present in bones and teeth. Calcium phosphates are easily synthesized, playing an important role in regenerative medicine, being able to be used as bone implants [1-6].

There are different ways of synthesizing phosphates, the most commonly used being wet chemical method. In this process the product obtained is suspended in the aqueous medium, so separation and subsequent drying are necessary. Different drying methodologies have been described in the literature, such as drying by evaporation concentration processes [7], drying in trays [8], freeze-drying [9] and spray drying [10-12], among others.

Drying influences particle size in most processes. On the other hand, the particle size determines in many cases the physical-chemical and biological properties of the material obtained. In the case of calcium phosphates and hydroxyapatite, it has been reported that its use as a biomaterial in bone regeneration is favored as the particle size is smaller. It has been reported that particle size in a nanometric form facilitates the adhesion, proliferation and differentiation of osteoblastic cells, which causes a greater rapidity in the bone regeneration process [3].

Previous work reported in our research group showed that the application of ultrasound during the calcium phosphate synthesis process decreases the particle size of these materials [7, 13]. On the other hand, these studies were linked to the application of different drying methodologies to evaluate the influence on particle size [7, 8, 13].

The objective of this work was to study the influence of the use of ultrasound and spray drying on the synthesis of amorphous calcium phosphate.

2. MATERIALS AND METHODS

Amorphous calcium phosphate synthesis (ACP).

Obtaining ACP was performed using the wet method [7]. Calcium hydroxide solution was heated to 80 ° C. Then, under constant stirring the phosphoric acid solution was added. Two variants of synthesis (without application of ultrasound and applying ultrasound) were studied. A Sonus Vibra Cell equipment, United States, (Pulse: 15s (active) and 3s (inactive); Amplitude: 30%) was used.

Once the reaction was completed, the supernatant liquid was separated. A suspension was prepared with a mixture of calcium phosphate precipitates and deionized water (10% total solids content). The suspension was vigorously stirred before and during spray drying to avoid particle agglomeration. It was subsequently atomized (Büchi 191 equipment, Switzerland) at a pressure of 600 L/h and a flow rate of 10 mL/min. The inlet and outlet temperatures of the nozzle were adjusted to 160 ° C and 70 ° C, respectively. The samples obtained were characterized.

X-ray powder diffraction studies.

The XRD spectra were recorded at room temperature (25 ºC) with a SIEMENS D5000, DIFFRAC PLUS XRD diffractometer (Germany) with BRAGG-Brentano geometry, Cu Kα radiation (λ=0.154 nm), Flicker detector and graphite monochromator. The scattering angle range from 4º to 80º with 2θ step interval of 0.02º was used. ACP samples were cut into small

pieces and laid on the glass sample holder, analyzed under plateau conditions. An operating voltage of 40 kV and current of 30 mA was utilized, and the intensities were measured in the range of 5° < 2θ < 30°. Peak separations were carried out using Gaussian deconvolution. The d-spacings were calculated using the Bragg equation. Crystallographic search match software was used to identify the crystal structure of samples.

FTIR spectroscopy.

FTIR spectra of the samples were measured on a FTIR - VERTEX 70 / BRUKER spectrometer (Germany). A total of 64 cumulative scans were taken, with a resolution of 4 cm^{-1}, in the frequency range of 4000 to 400 cm^{-1}, in transmission mode.

Scanning Electron Microscopy.

Scanning electron microscopy (SEM) imaging of ACP was carried out using a FEG-MEV; JEOL 7500F scanning electron microscope (Germany). The equipment was operated at an acceleration voltage of 2 kV. The samples were coated by carbon evaporation (Baltec SCD 050 Spputer Coater, USA).

Particle size by scanning electron microscopy was determined. Five SEM images at magnifications X100000 were evaluated. In each images, five random measurements of the particle size were performed. With the data obtained, the mean particle size was determined.

Calcium determination.

The calcium content by atomic absorption spectrometry was determined. Spectr AA-50 (VARIAN, USA) equipment (calcium hollow cathode lamp, air-acetylene gases, 422.7 nm wavelength and 10A current) were used.

0.25 g of samples were weighed and transferred to a 500 mL volumetric flask. 5 mL of hydrochloric acid and 100 mL of water were added. It was stirred in a circular manner until the sample was dissolved and brought to volume with distilled water. 2 mL of the solution was transferred to a 50 mL volumetric flask, 3 mL of 5.8% lanthanum oxide solution was added and brought to volume with distilled water. Calcium concentrations were determined.

A calibration curve with calcium concentrations (calcium carbonate (NIST SRM 915b) dried at 250 ° C for 2 h) between 2 and 14 ppm was prepared.

Statistical analysis.

Statistical analysis using one way ANOVA was applied [14, 15]. A confidence level of (1-α) = 95% and a significance of α = 5% was used. All data were processed using the statistical software InfoStat (2017 version).

3. RESULTS

Figure 1 shows the X-ray diffractograms of the samples (not treated and treated with ultrasound). The presence of OCP, hydroxyapatite (HA), monohydrogen calcium phosphate dihydrate (DCPD) and calcium deficient hydroxyapatite (Had), characteristic of ACP type apatite [16] was observed. The main indices (*h k l*) for ACP are indicated on the spectra according to powder diffraction file (PDF 00-011-0293; PDF 01-074-1301; PDF 00-009-0432)

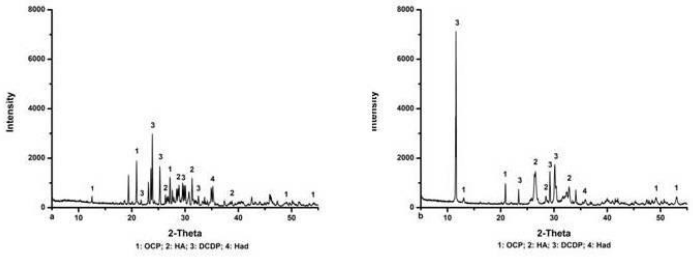

Figure 1. X-ray diffractogram. (a: Rx analysis of ACP synthesized without ultrasound and b: Rx analysis of ACP synthesized with ultrasound).

The presence of an intense peak at 2Θ = 11.6 that corresponds to DCPD in the sample synthesized with ultrasound application was observed in the X-ray diffractogram. Similar results to those reported by Pelizaro *et al*, [13].

During the ACP synthesis, an induction process affected by pH and temperature occurs, with a subsequent hydrolysis process, generating a mixture of different phosphate phases, including DCPD phase, unstable and poorly soluble intermediate, which tends to precipitate easily [17].

This process is favored by the application of ultrasound, stimulating the reactivity of the chemical species involved in the process. Studies reported by Kim *et al*, [18] showed that when applying ultrasound during the synthesis of hydroxyapatite from phosphoric acid and calcium hydroxide, in the first minutes the formation of DCDP predominates as a typical intermediate of this acid base reaction.

Figure 2 shows the FTIR spectrum of the synthesized samples. Bands at 1120, 1026, 559 and 515 cm-1 characteristic to the presence of phosphate groups were observed. On the other hand, a band appears at 890 cm-1 due to the presence of PO_4^{3-} ions.

Peaks at 1408, 1343 (asymmetric stretch vibration) and 882,1 cm^{-1} (out-of-plane bend vibration) characteristic of the CO_3^{2-} group were observed. These peaks indicate the presence of type A and type B carbonated hydroxyapatite in the samples.

Scanning electron microscopy showed in both cases that the morphology of the product obtained is spherical, with a rough surface with small crystalline particles (Figure 3). The literature reports that spray-dried hydroxyapatite generally has a spherical morphology, with a rough surface that has nanocrystalline particles [10]. The results obtained coincide with what was reported.

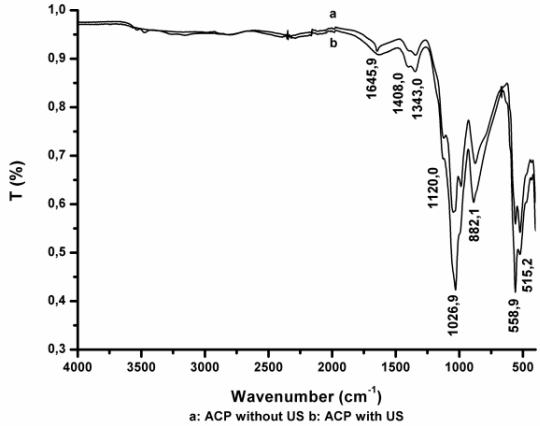

Figure 2. FTIR spectra. (a: FITR analysis of ACP synthesized without ultrasound and b: FITR analysis of ACP synthesized with ultrasound).

The particle size determination showed that for the samples synthesized without ultrasound application the average particle size was 85.1 ± 6.9 nm (between 261 and 32 nm). While the sample synthesized by applying ultrasound, the average particle size was 36.1 ± 1.1 nm (between 58.7 and 21.1 nm), showing in this case a more homogeneous distribution of the same (Figure 4). Statistical analysis showed significant differences between particle size ($p = 0.0156$) for a level of 0.05.

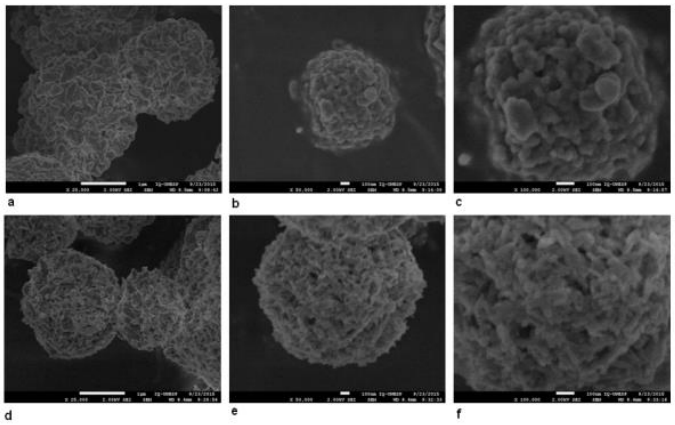

Figure 3. Results of analysis by SEM. ACP synthesized without ultrasound (a: 25000X; b: 50000X and c: 100000X). ACP synthesized with ultrasound (d: 25000X; e: 50000X and f: 100000X).

The application of ultrasound decreases the particle size, increasing the surface area, which favors the spray drying process. Studies reported in the literature have shown that the application of ultrasound during the synthesis process allows the decrease in particle size in the synthesized material [7, 19, 20]. Poinern *et al*. [19] reported a decrease in particle size to values around 30 nm, while Giardine *et al*. [20] reached values between 31.7 and 70.6 nm. Pelizaro *et al*. [13] demonstrated that better results were achieved when applying ultrasound during the synthesis process than when applied after the synthesis process.

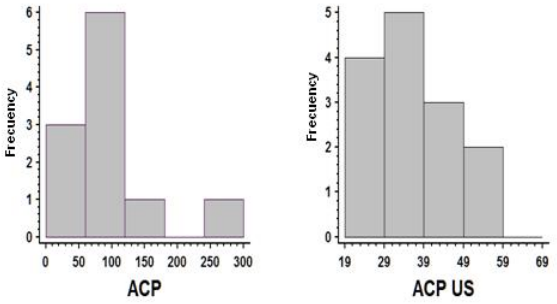

Figure 4. Histogram of the particle size distribution measured by MEV at magnification 100000X.

The results achieved showed that the particle size decreased, obtaining values similar to those reported in the literature. On the other hand, spray drying favors rapid drying of the sample.

Finally, the determination of the calcium content by atomic absorption (calibration curve: $y = 0.0046X + 0.00$, $R2 = 99.7\%$) was 67.3 ± 3.6 and 69.4 ± 2.4 for ACP and US ACP, respectively. The statistical comparison showed that there were no significant differences between them.

The calcium content in the samples evaluated is within the range of values reported by different authors for amorphous calcium phosphates synthesized by wet chemical method [7, 13, 21, 22].

4. CONCLUSIONS

The results of this study demonstrate that amorphous calcium phosphate synthesized by wet chemical methods can be spray dried by obtaining a material with small granolumetry. When ultrasound is applied during the synthesis, the particle size decreases significantly, which causes an increase in surface area, favoring the drying process.

5. REFERENCES

1. Black, C.R.M.; Goriainov, V.; Gibbs, D.; Kanczler, J.; Tare, R.S.; Oreffo, R.O.C. Bone tissue engineering. *Curr. Mol. Biol. Reports*. **2015**, *1*, 132–140, https://doi.org/10.1007/s40610-015-0022-2.

2. Zhao, J.; Liu, Y.; Sun, W.; Yang, X. First detection, characterization and application of amorphous calcium phosphate in dentistry. *J. Dent. Sci*. **2012**, *7*, 316–323, https://doi.org/10.1016/j.jds.2012.09.001.

3. Lotsari, A.; Rajasekharan, A.K.; Halverson, M.; Andersson, M. Transformation ofamorphous calcium phosphate to bone-like apatite. *Nat. Commun*. **2018**, *9*, https://doi.org/10.1038/s41467-018-06570-x.

4. Chen, Z.; Liu, Y.; Mao, L.; Gong, L.; Sun, W.; Feng, L. Effect of cation doping on the structure of hydroxyapatite and the mechanism of defluoridation. *Ceram Int* **2018**, *44*, 6002–6009, https://doi.org/10.1016/j.ceramint.2017.12.191.

5. Ghahremani, D.; Mobasherpour, I.; Salahi, E.; Ebrahimi, M.; Manafi, S.; Keramatpour, L. Potential of nano crystalline calcium hydroxyapatite for Tin(II) removal from aqueous solutions: equilibria and kinetic processes. *Arab J Chem*, **2017**, 10, S461–S471, https://doi.org/10.1016/j.arabjc.2012.10.006.

6. Tite, T.; Popa, A.C.; Marinela Balescu, L.; Maria Bogdan, I.; Pasuk, I.; Ferreira, J.M.F.; Stan, G.E. Cationic Substitutions in Hydroxyapatite: Current Status of the Derived Biofunctional Effects and Their In Vitro Interrogation. Methods. *Materials (Basel)*. **2018**, *11*, 2081, https://doi.org/10.3390/ma11112081.

7. Rodríguez-Chanfrau, J.E.; Garcia, P.T.A.; Silva, R.M.; Tolaba, A.G.; Pizoni, E.; Veranes-Pantoja, Y.; Guastaldi, A.C. Synthesis by wet chemical method of different phases of apatites applying ultrasound. *Journal of Bionanoscience* **2018**, *12*, 134-141, https://doi.org/10.1166/jbns.2018.1502.

8. Pelizaro, T.A.; Rodriguez-Chanfrau, J.E.; Guastaldi, A.C. Evaluation of tray drying on the particle size in the synthesis of three phases apatites. Annals of 14 Congresso da Sociedade Latino Americana de Biomateriais, *Orgãos Artificiais e Engenharia de Tecidos-SLABO. 5a Edição do Workshop de Biomateriais, Engenharia de Tecidos e Orgãos Artificiais-OBI, Metallum Eventos Técnico e Científicos, Sao Paulo*. **2017**, 140–146.

9. Debone, P.R.; Pelizaro, T.A.G.; Rodriguez-Chanfrau, J.E.; Almirall, La S.A.; Veranes-Pantoja, Y.; Guastaldi, A.C. Calcium phosphates nanoparticles: The effect of freeze-drying on particle

size reduction *Materials Chemistry and Physics* **2020**, *239*, 122004, https://doi.org/10.1016/j.matchemphys.2019.122004.
10. Bastan, F.E.; Erdogan, G.; Moskalewicz, T.; Ustel, F. Spray drying of hydroxyapatite powders: The effect of spray drying parameters and heat treatment on the particle size and morphology. *Journal of Alloys and Compounds.* **2017**, *724*, 586-596, https://doi.org/10.1016/j.jallcom.2017.07.116
11. Luo, P.; Nieh, T.G. Synthesis of ultrafine hydroxyapatite particles by a spray dry method. *Materials Science and Engineering: C*. **1995**, *3*, 75-78, https://doi.org/10.1016/0928-4931(95)00089-5.
12. Wang, A.; Lu, Y.; Zhu, R.; Li, S.; Ma, X. Effect of process parameters on the performance of spray dried hydroxyapatite microspheres. *Powder Technol*. **2009**, *191*, 1–6, https://doi.org/10.1016/j.powtec.2008.10.020.
13. Pelizaro, T.A.G.; Tolaba, A.G.; Rodriguez-Chanfrau, J.E.; Veranes-Pantoja, Y.; Guastaldi, A.C. Influence of the application of ultrasound during the synthesis of Calcium Phosphates. *Journal of Bionanoscience*. **2018**, *12*, 733-738, https://doi.org/10.1166/jbns.2018.1585.
14. Montgomery, D.C. *Design and analysis of experiments*, 9th edition.; Wiley, USA, 2017; pp. 65-130.
15. Flores-Ruiz, E.; Miranda-Novales, M.G.; Villasís-Keever, M.A. The research protocol VI: How to choose the appropriate statistical test. Inferential statistics. *Rev Alerg Mex*. **2017**, *64*, 364-370, https://doi.org/10.29262/ram.v64i3.304.
16. Perez, P.V. *Estudo da solubilidade de apatitas em meios de interesse biológico.* Dissertação de Mestrado. Instituto de Química. Universidade Estadual Paulista. UNESP. Araraquara, Sao Paulo, Brazil. 2012.
17. Dorozhkin, S.V. Nanosized and nanocrystalline calcium orthophosphates. *Acta Biomater*. **2010**, *6*, 715–734, http://dx.doi.org/10.1016/j.actbio.2009.10.031.
18. Kim, W.; Saito, F. Sonochemical synthesis of hydroxyapatite from H_3PO_4 solution with $Ca(OH)_2$. *Ultrasonics Sonochemistry.* **2001**, 8, 85-88, https://doi.org/10.1016/S1350-4177(00)00034-1.
19. Poinern, G.E.; Brundavanam, R.K.; Mondinos, N.; Jiang, Z.T. Synthesis and characterization of nanohydroxyapatite using an ultrasound assisted method. *Ultrason. Sonochem.* **2009**; *16*, 469-74, https://doi.org/10.1016/j.ultsonch.2009.01.007.
20. Giardina, M.A.; Fanovich, M.A. Synthesis of nanocrystalline hydroxyapatite from $Ca(OH)_2$ and H_3PO_4 assisted by ultrasonic irradiation. *Ceram. Int.* **2010**, *36*, 1961-1969, https://doi.org/10.1016/j.ceramint.2010.05.008.
21. Markovic, M.; Fowler, B.O.; Tung, M.S. Preparation and Comprehensive Characterization of a Calcium Hydroxyapatite Reference Material. *J. Res Natl. Inst. Stand. Technol.* **2004***; 109*, 553-568, https://doi.org/10.6028/jres.109.042.
22. Gonzalo Sequeda, L.; Milciades Díaz, J.; Gutiérrez, S.J.; Perdomo, S.J.; Gómez, O.L. Synthetic hydroxyapatite obtaining using three different methods and characterization to use it as bone substitute. *Rev. Colomb. Cienc Quím Farm.* **2012**, *41*, 50-66, https://doi.org/10.15446/rcciquifa.

6. ACKNOWLEDGEMENTS

The authors are grateful to the CAPES-MES Project for the support to carry out this work (project 186/13), the X-ray laboratory and the scanning electron microscopy laboratory of the Chemistry Institute of UNESP. Araraquara, Brazil.